Supplementary Materials

AIE-active tetraphenylethene functionalized silver-tetrazolate coordination polymer for selective fluorescence sensing of explosives

Hai-Peng Kang,[a] Han-Chen Zhou,[a] Xiong Tang,[a] Chang Liu,[a] Yong-Hua Li,*[a] Hao-Zhe Zhang,[a] Jian Su,*[b] Marilena Ferbinteanu*[c], Hua-Yu Wu[a] and Shi Wang*[a]

[a] State Key Laboratory of Organic Electronics and Information Displays & Institute of Advanced Materials (IAM), Nanjing University of Posts & Telecommunications, Nanjing 210023, People's Republic of China.
E-mail: iamswang@njupt.edu.cn; iamyhli@njupt.edu.cn
[b] School of Chemistry and Chemical Engineering, Nanjing University of Science and Technology, Nanjing, Jiangsu 210094, People's Republic of China.
E-mail: sujian@njust.edu.cn
[c] Faculty of Chemistry, University of Bucharest, Dumbrava Rosie 23, Bucharest 020462, Romania. E-mail: marilena.cimpoesu@g.unibuc.ro

Experimental Section

Materials and Measurements

All chemical reagents were obtained from commercial sources and used without further purification unless otherwise noted. All synthetic procedures were performed under a nitrogen atmosphere by standard Schlenk techniques. H$_4$ttazpe was prepared using a modified method according to the previous report of our group. Fluorescence analysis was carried out on RF-6000. The FTIR spectra were measured using a Vector 22 Fourier transform infrared spectrometer. Thermogravimetric analysis (TGA) was performed under N$_2$ atmosphere on a DTG-60A shimadzu instrument and heated at a rate of 10 °C/min. UV-Vis spectra were recorded on a UV-Vis spectrophotometer (UV-3600). The XRD was performed by a Bruker D8-advance X-ray diffractometer

using monochromatic CuK$_\alpha$ radiation. NMR spectra were recorded on Bruker-400 MHz in CDCl$_3$ and CD$_3$OD as internal standard with TMS. The chemical shift values are reported in ppm (δ) and coupling constants are reported in Hertz. Single-crystal diffraction data for LMOF-**1** were collected at 100K on a Smart Brucker CCD area detector diffractometer using a graphite monochromator with K$_\alpha$ radiation (λ =0.71073 Å). Cell parameters were retrieved using SMART software and refined using SAINT on all observed reflections. Data reductions were performed using the SAINT software, and absorption corrections were applied using SADABS supplied by Bruker. [1] The structures were solved by direct methods and refined to convergence by full-matrix least squares on F^2 with anisotropic thermal parameters for all non-hydrogen atoms by SHELXTL (Bruker, 2008) and SHELXL-2016/6 (Sheldrick, 2016).[2] Hydrogen atoms were placed in idealized positions using a riding model. The topological analysis was performed with the ToposPro program package and the Topological Types Database-TTD collection of periodic network topologies.[3] Crystallographic data for the structures have been deposited at the Cambridge Crystallographic Data Centre, CCDC-2181308 for LMOF-**1**. These data can be obtained free of charge (http://www.ccdc.cam.ac.uk/data_request/cif).

Synthesis of tetrakis(4-cyanophenyl)ethylene (TPE-CN$_4$)

A mixture of 1,1,2,2-tetrakis(4-bromophenyl)ethane (TPE-Br$_4$, 4.00 g, 6.2 mmol) and CuCN (4.5 g, 49.6 mmol) in dry DMF (25 mL) was heated at reflux under nitrogen for two days. Ammonia (25 mL) and water (45 mL) were added to the reaction mixture after cooling to the room temperature. The product was extracted with dichloromethane (3 × 100 mL) and the organic layer dried over sodium sulfate, filtered, and evaporated. A quantity of 3.5 g (88 %) of TPE-CN$_4$ was isolated as yellow powder. ^{1}H NMR (400 MHz, CDCl$_3$) δ 7.48 (t, J = 8.2 Hz, 1H), 7.08 (d, J = 8.2 Hz, 1H).

Synthesis of tetrakis[4-(1H-tetrazol-5-yl)phenyl]ethylene (H$_4$ttazpe)

To a solution of sodium azide (3.8 g, 58 mmol) and zinc bromide (7.9 g, 58 mmol) in water (20 mL) and 2-propanol (10 mL) was added TPE-CN$_4$ (2.5 g, 5.8 mmol). The reaction was heated at reflux under nitrogen for two days. The resulting mixture was added 1M NaOH to pH=10 and then filtered. The filtrate was collected and adjust the pH value to 5-6 with 1 M HCl. The mixture was filtered to give the crude product which was purified by Column Chromatography (CH$_3$OH:Ethyl Acetate=1:2) to yield a yellow powder 2.4 g (70 %). ^{1}H NMR (400 MHz, CD$_3$OD) δ 7.85 (d, J = 8.3 Hz, 8H), 7.30 (d, J = 8.4 Hz, 8H).

Caution! Metal azides are water sensitive and potentially explosive and should be handled with care.
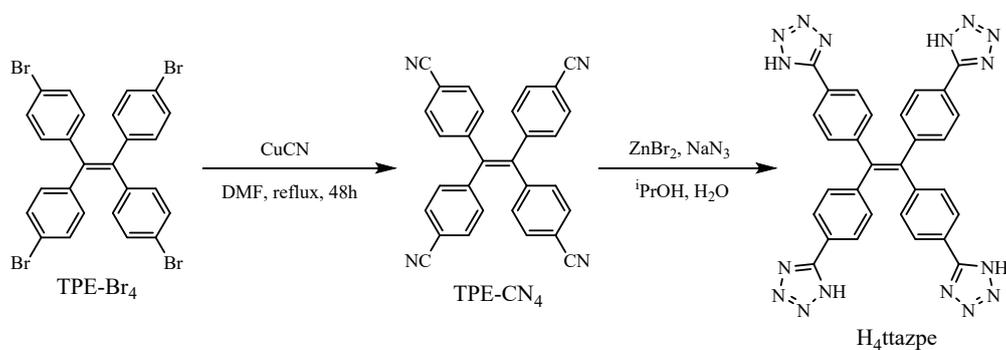
Scheme S1. Synthesis of H$_4$ttazpe ligand.

(a)
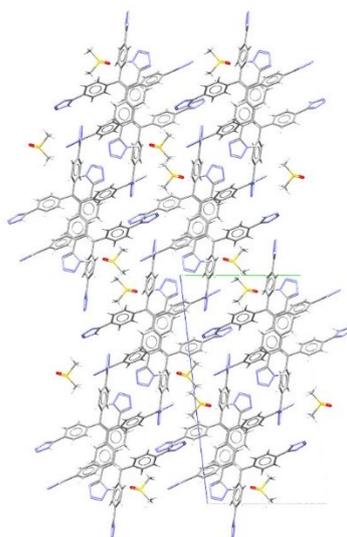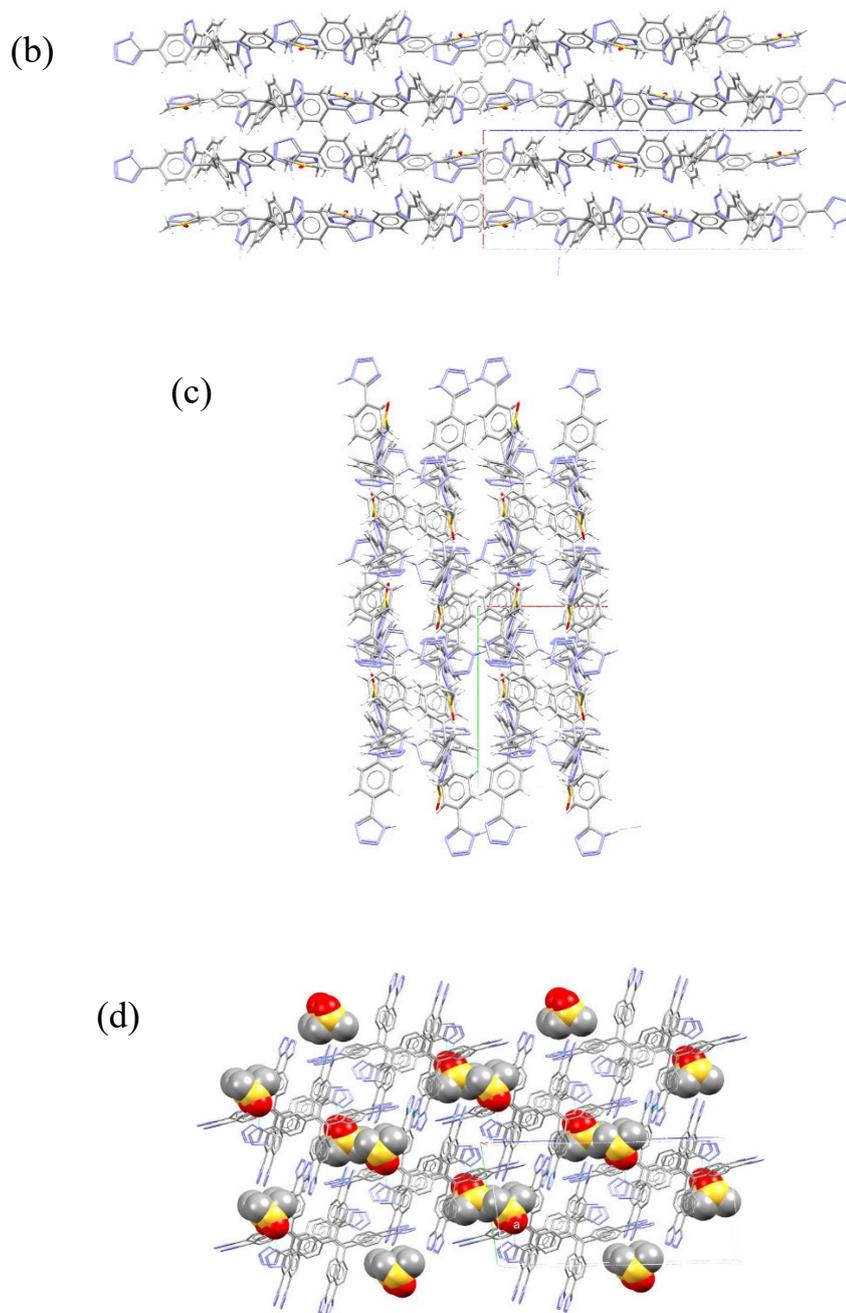
Figure S1. (a) The crystal packing diagram for $H_4ttazpe$ along a axis. (b) Packing diagram along b axis. (c) Packing diagram along c axis. (d) Packing diagram along *b* axis showing the DMSO channels.
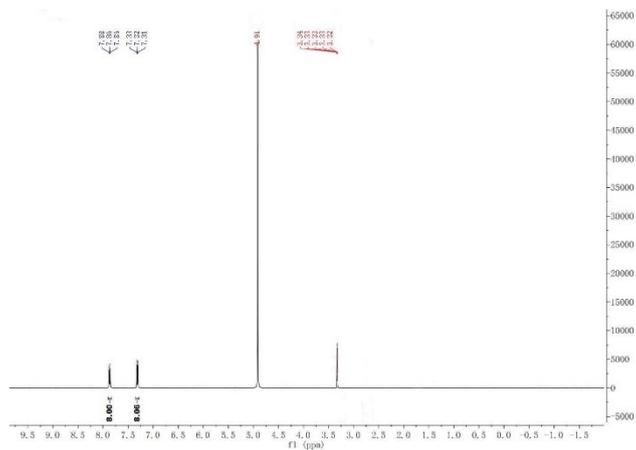
Figure S2. ^{1}H NMR spectrum of H$_4$ttazpe ligand.
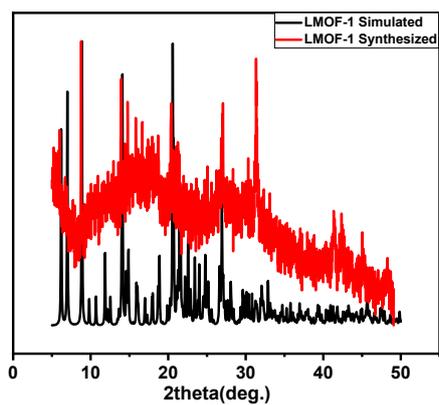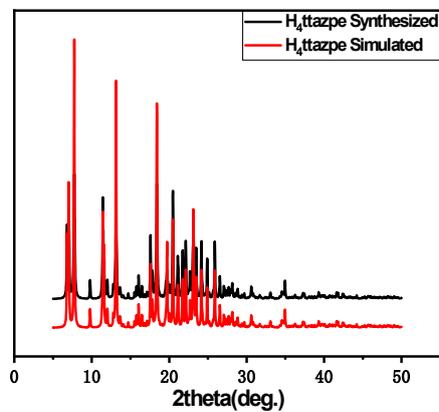
Figure S3. PXRD patterns of as-synthesized H$_4$ttazpe ligand and LMOF-**1**.
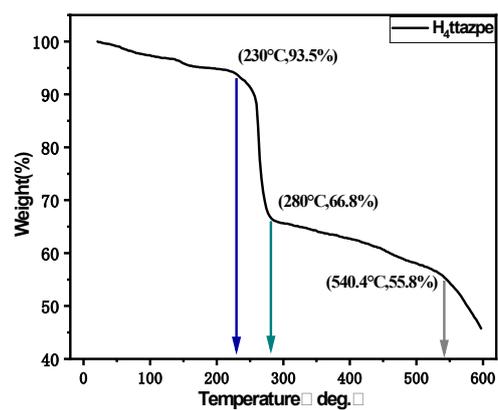
Figure S4. TGA of H$_4$ttazpe ligand.

(a)

(b)

(c)
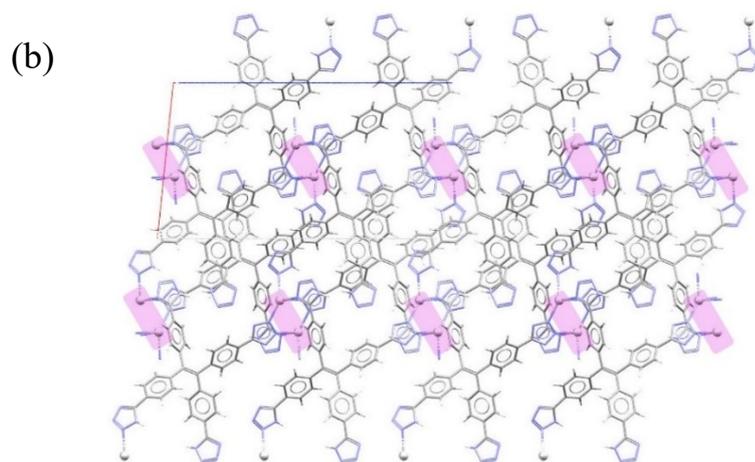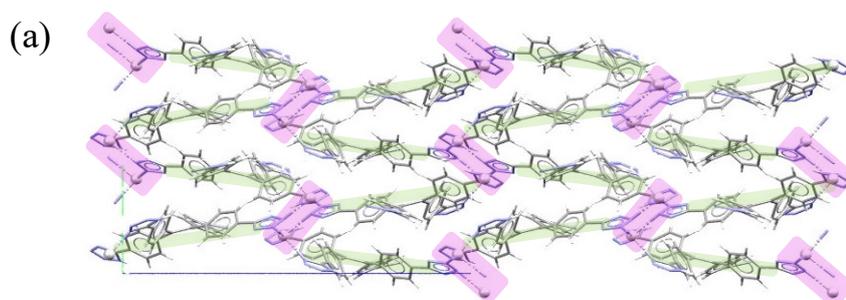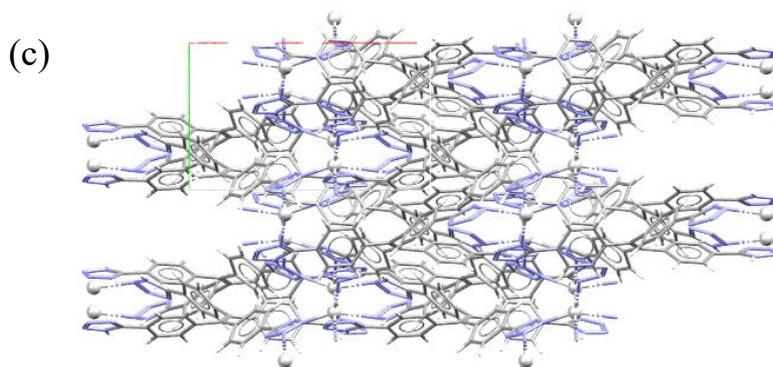
Figure S5. (a) Packing diagram of LMOF-1 along a axis showing the {Ag$_2$} nodes in pink and bridging ligands in green. (b) Packing diagram along b axis. (c) Packing diagram along c axis.

Cluster representation of net topology

The cluster simplification procedure implemented in ToposPro allows to identify more complex building units of a structure and characterize their connection mode. The topology of underlying net of LMOF-1 in cluster representation is **rtl** (Fig. S6a, top). This is a binodal 3,6-coordinated net with point symbol is $(4.6^2)_2(4^2.6^{10}.8^3)$. The identified structure building units, which serve as nodes of the underlying net are Ag$_2$C$_2$N$_8$ cluster (Fig. S6a, bottom right, ZE) and 3-coordinated carbon atom of the ligand (Fig. S6a, bottom left, ZD).
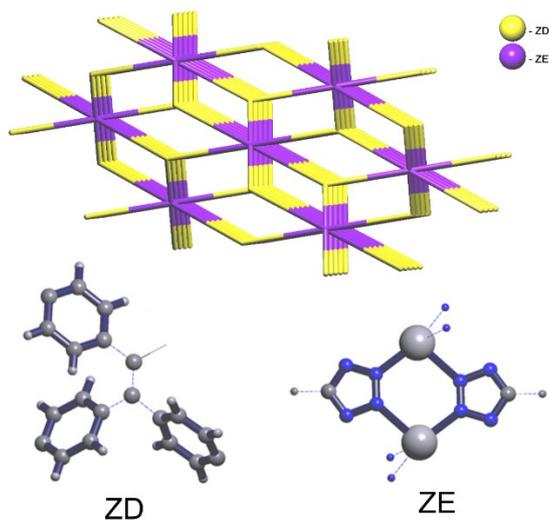
Figure S6a. The underlying net in the cluster All Nodes representation (top) with **rtl** topology. ZD and ZE nodes correspond to C and Ag$_2$C$_2$N$_8$ structure building units (bottom left and right).

Standard representation of net topology

In a standard simplified procedure, ligands are represented as their centers of mass, while their bonds with metal atoms are retained. This makes it possible to clearly demonstrate the method of bonding a metal with ligands in the framework. The net in the standard representation of LMOF-1 has a **crb** topology (Fig. S6b). This is a 4-coordinated uninodal net with point symbol (4.6^5).
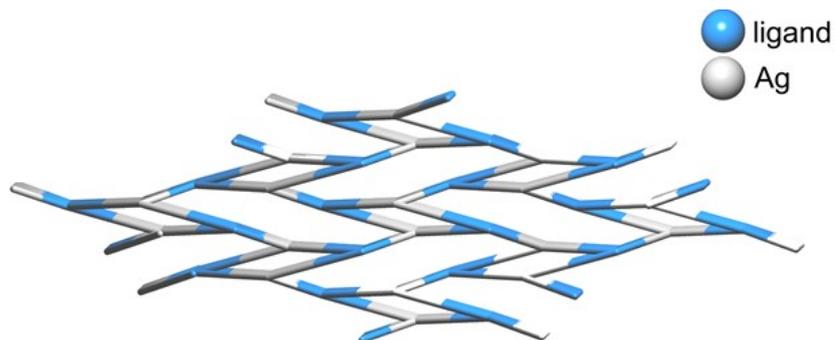
Figure S6b. The underlying net of **crb** topological type in standard representation of the valence-bonded MOF.
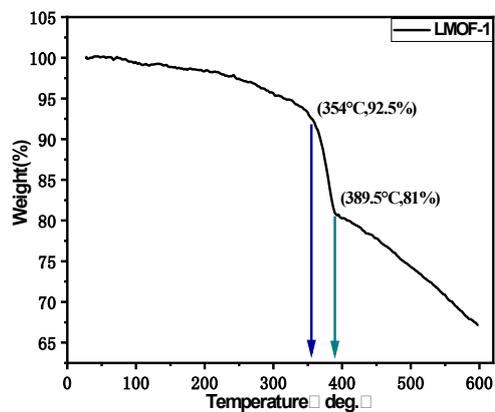
Figure S7. TGA of LMOF-**1**.
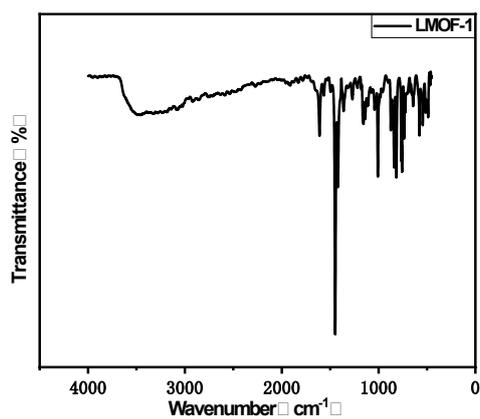
Figure S8. IR of LMOF-**1**.
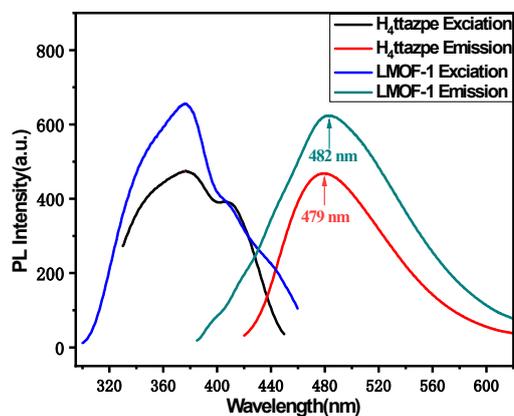
Figure S9. Emission and exciation spectra of H$_4$ttazpe and LMOF-**1** in the solid state.
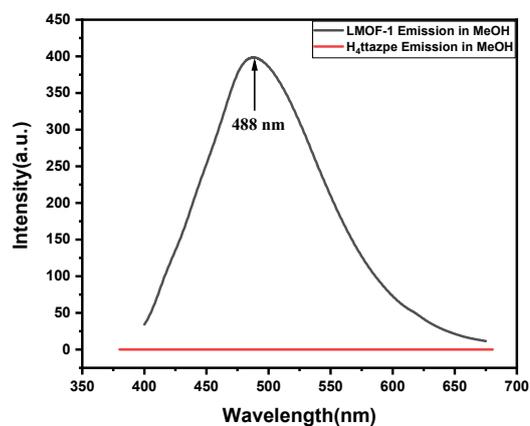
Figure S10. Emission spectra of H$_4$ttazpe and LMOF-**1** in MeOH (3mg/3mL).
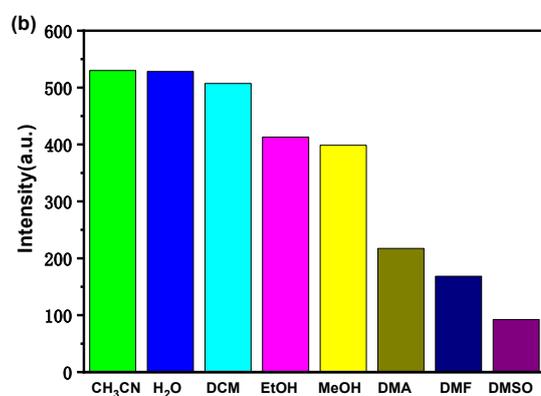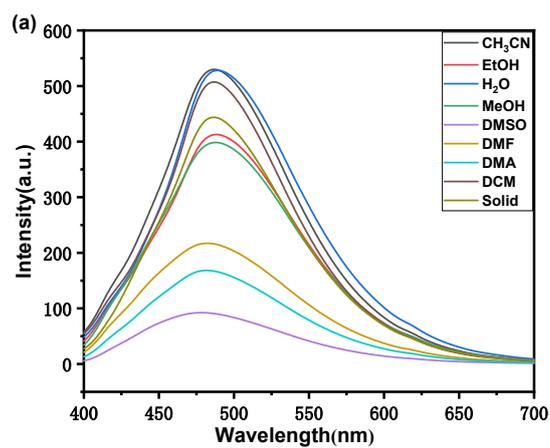
Figure S11. (a) Fluorescence spectra and (b) Changes in the fluorescence intensity of LMOF-**1** in different organic solvents.
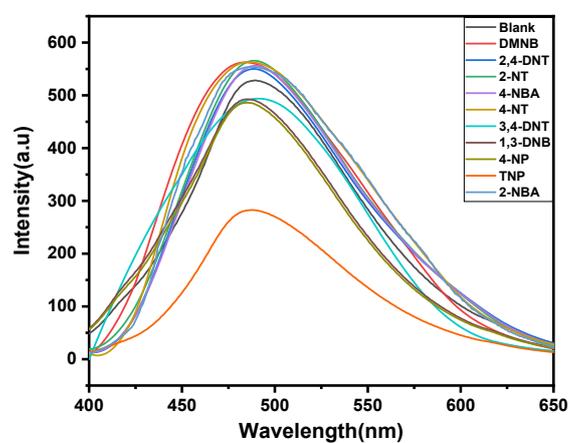
Figure S12. The fluorescence spectrum of LMOF-**1** with different nitroaromatic explosives at 6.62×10^{-5} M concentration.
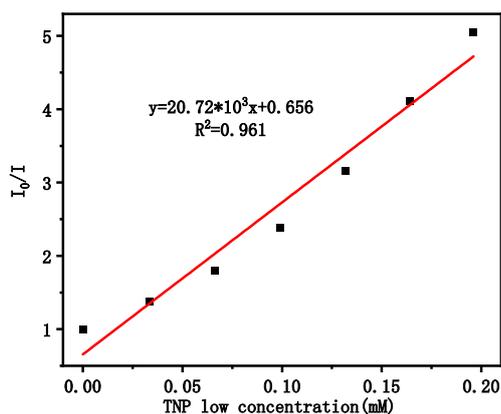
Figure S13. Stern-Volmer plot of relative fluorescence intensity and TNP concentration at low concentration.

$$\frac{I_0}{I} = 1 + K_{SV}[C]$$
（1）

$$C = （10mM * V）/（3mL + V）$$
（2）

[C]：TNP concentration in suspension; V：Volume of TNP in suspension; I_0、I：Fluorescence intensity of suspension before and after the addition of TNP; Ksv：Quenching constant.

(a)   (b)
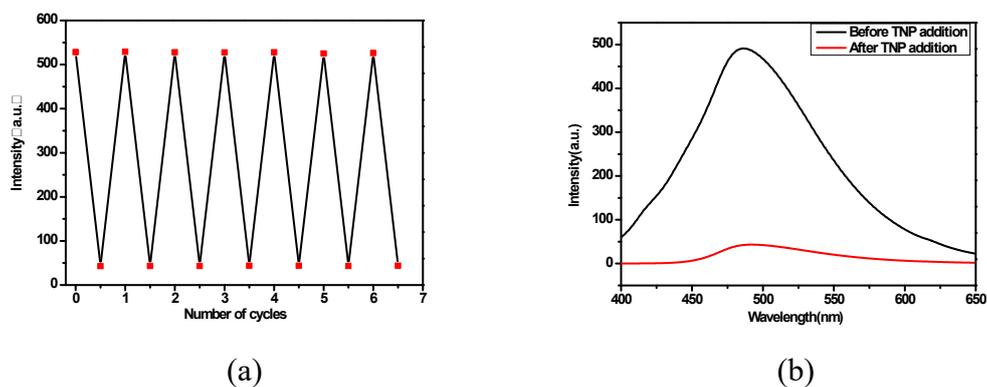
Figure S14. (a) Recycling of fluorescence quenching of LMOF-**1** by TNP; (b) Fluorescence spectra before and after the seventh quenching.

Table S1. Crystallographic and refinement data for the reported structure of LMOF-**1**.

Crystal data	LMOF-**1**
Empirical formula	$C_{30}H_{19}AgN_{16}$
Formula weight	711.48
Crystal system	monoclinic
Space group	$P\,2_1/c$
a (Å)	14.312(16)
b (Å)	8.755(10)
c (Å)	25.39(3)
α (°)	90
β (°)	95.79(2)
γ (°)	90
Volume (Å³)	3165(6)
Z	4
$D_{calc.}$(g/cm³)	1.493
F(000)	1432
μ MoKα (mm⁻¹)	0.686
Range of h, k, l	−17/16, −8/10, −30/26
θ min/max	1.43 / 25.00
Data/restraints/parameters	5560/0/429
Goodness of fit on F^2	1.050
Final R indices [I>2σ(I)]	R_1=0.0514 wR_2=0.1132
R indices (all data)	R_1=0.1042 wR_2=0.1477

$R_1 = \sum||F_o|-|F_c||/\sum|F_o|.$ $wR_2 =[\sum w(F_o^2-F_c^2)^2/\sum w(F_o^2)]^{1/2}$

Table S2. Selected bond lengths (Å) and bond angles (º) for LMOF-**1**.

配合物 LMOF-**1**			
N7−Ag1²	2.463(5)	N9−N10−Ag1³	115.4(3)
N10−Ag1³	2.614(5)	N11−Ag1−N16	125.67(16)
N11−Ag1	2.300(5)	N11−Ag1−N7⁴	142.01(17)
Ag1−N16	2.429(5)	N16−Ag1−N7⁴	91.71(15)
Ag1−N7⁴	2.463(5)	N11−Ag1−N10³	100.22(16)
Ag1−N10³	2.614(5)	N16−Ag1−N10³	88.89(15)
N11−N10−Ag1³	127.9(3)	N7⁴−Ag1−N10³	85.48(15)

Symmetry transformations used to generate equivalent atoms:¹+X, 1/2-Y, 1/2+Z; ²1+X, +Y, +Z; ³1-X, 1/2+Y, 1/2-Z; ⁴-1+X, +Y, +Z; ⁵1-X, -1/2+Y, 1/2-Z; ⁶+X, 1/2-Y, -1/2+Z

References

(1) (a) SAINT-plus, Version 6.02, Bruker Analytical X-ray System, Madison, WI, **1999**; (b) Sheldrick, G. M. *SADABS, an Empirical Absorption Correction Program, Bruker Analytical X-ray Systems, Madison, WI*, **1996**

(2) Sheldrick, G. M. A short history of SHELX. *Acta. Crystallogr. Sect. A: Found Crystallogr*. **2008**, *64*, 112.

(3) (a) Blatov, V. A.; Shevchenk, A. P.; Proserpio, D. M. Applied topological analysis of crystal structures with the program package ToposPro, *Cryst. Growth. Des.* **2014**, *14,* 3576. (b) Alexandrov, E. V.; Blatov, V. A.; Kochetkov, A. V.; Proserpio, D. M. Underlying nets in three-periodic coordination polymers: topology, taxonomy and prediction from a computer-aided analysis of the Cambridge Structural Database. *CrystEngComm.* **2011,** *13,* 3947.